Analysis of Transient Recovery Voltage in 400 kV SF$_6$ Circuit Breaker Due to Transmission Line Faults

Božidar Filipović-Grčić[1], Ivo Uglešić[1], Dalibor Filipović-Grčić[2]

Abstract – *Transient recovery voltage (TRV) is calculated according to the IEC standards and using the EMTP-ATP software. Modeling of electric arc for the SF$_6$ circuit breaker is presented. Influence of grading capacitors and line bay disposition on the TRV waveform on the side of the line in a 400 kV substation is analyzed for the short-line fault (SLF) conditions. Fault location at which the rate of rise of recovery voltage (RRRV) is the highest was determined using the EMTP-ATP simulations. Results obtained according to the IEC standards and using the EMTP-ATP are compared. Copyright © 2011 Praise Worthy Prize S.r.l. - All rights reserved.*

Keywords: Transient Recovery Voltage, Short-Line Fault, SF$_6$ Circuit Breaker, Electric Arc Model, EMTP Simulations

Nomenclature

v	Arc voltage
i	Arc current
g	Arc conductance
$P(g)$	Arc cooling power
$T(g)$	Arc thermal constant
g_0	Initial arc conductance
α, β	Arc constants
Δt	Simulation time step

I. Introduction

TRV is the voltage across the opening contacts of a fault-interrupting circuit breaker (CB) immediately after the electric arc is extinguished [1]. This voltage may be considered in two successive time intervals: one during which the transient voltage exists, followed by the second one during which the power frequency voltage exists alone.

For TRV studies, the two most important factors are: the maximum voltage attained depending on the normal system operating voltage and the RRRV during oscillation, which is also dependent on the frequency of oscillations [2]-[5]. The impact of the line bay disposition on the TRV waveform on the side of the line in a 400 kV substation is analyzed in the SLF conditions. A comparison of results obtained from calculations conducted according to the IEC standards [6] and using the EMTP-ATP software is done.

The influence of various parameters on TRV is analyzed: stray capacitances of the voltage instrument transformers; distance from the fault location to the CB; capacitors in parallel with CB poles; electric arc modeling.

II. Short-Line Fault

Occurrence of a fault on the overhead line relatively close to a CB is characterized by the TRV oscillation from the line side. This oscillation is caused by a short length of the line between the CB and the place of the fault. In the transitional period of establishing TRV on the line side to the first peak, which lasts several microseconds, there is a danger of occurrence of thermal breakdown in the SF$_6$ CB. The IEC standards define the procedure for the determination of TRV on the line side when the CB is tested in SLF conditions.

Information about TRV that a CB is expected to encounter in service is of great importance in its design and operation. Triangular-shaped TRVs are associated with SLF after current interruption and the line side voltage exhibits the characteristic triangular waveform. The rate of rise of the saw-tooth shaped TRV is a function of the line surge impedance and it is generally higher than that experienced with exponential or oscillatory TRVs. However, the TRV peak is generally lower. Because overhead lines have distributed electrical parameters (series resistance and inductance and shunt conductance and capacitance), the line side voltage oscillates in the form of a travelling wave with positive and negative reflections at the open breaker and at the fault location, respectively. Fig. 1 shows the line side component of TRV, which has a saw-tooth shape and the recovery voltage on the source side that rises much more slowly. Only the line side triangular recovery voltage is important during the early portion of the TRV [7].

The closer the fault to the CB, the higher the initial rate of rise of the line side recovery voltage due to the higher fault current, while the crest magnitude of this line side triangular wave decreases due to the shorter time needed for the reflected wave to return. The

amplitude and the rate of rise of TRV for these short-line faults are determined on a single-phase basis during their early time periods (typically less than 20 μs), when the source side voltage changes only slightly.
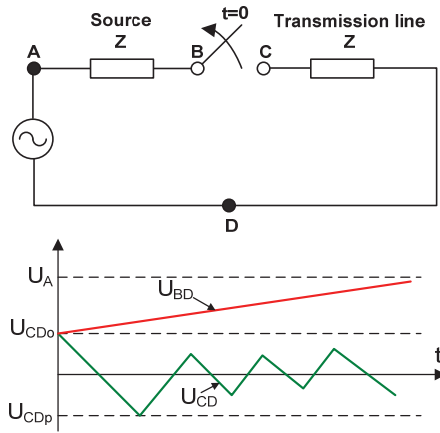

Fig. 1. TRV waveform for SLF (U_{BD} – source side voltage, U_{CD} – line side voltage)

III. Electric Arc Model for SF$_6$ Circuit Breaker

For calculation of the initial part of TRV, the modeling of the arc resistance in a SF$_6$ CB is important, because it has a significant impact on the TRV. Black box models use a mathematical description of the electrical behavior of an electrical arc. These types of models do not give full representation of the physical processes taking place inside the CB [8]. Recorded voltage and current traces during the "thermal period" are used to obtain the CB parameters that are later on substituted in differential equations. The most basic Cassie-Mayr equation is often used, as well as its modifications from the Schwarz-Avdonin model (1):

$$\frac{1}{g} \cdot \frac{dg}{dt} = \frac{1}{T(g)} \cdot \left[\frac{u \cdot i}{P(g)} - 1 \right] \quad (1)$$

Calculation of the arc conductance requires data on the cooling power and the thermal time constant. Parameters $P(g)$ and $T(g)$ are conductance dependent. The cooling power P and the thermal time constant T depend on temperature, CB type and design, and they can be defined as a function of conductance (2), (3):

$$T(g) = T_0 \cdot g^\alpha = 1.5\mu s \cdot g^{0.17} \quad (2)$$

$$P(g) = P_0 \cdot g^\beta = 4MW \cdot g^{0.68} \quad (3)$$

where α and β are constants whose values are given in Fig. 2. Arc equation could be solved if a sufficiently small time interval (Δt) can be observed in which P and T are constant. The differential equation (1) was solved

numerically with the Euler method for differential equations of the first order (4):

$$g(t + \Delta t) = g(t) + \left(\frac{i^2}{P_0 \cdot g(t)^\beta} - g(t) \right) \cdot \left(1 - e^{\frac{-\Delta t}{T(g)}} \right) \quad (4)$$

Depending on the difference between input (power) and cooling thermal energy (power loss), the arc temperature (and conductivity) is either going to increase or decrease. The test circuit described in [9] is shown in Fig. 2. The first step in solving equation (4) is to find solutions to the network equations (in EMTP) with the initial conductance value $g_0 = g(t_0)$. The solution to these equations gives the value for the current $i(t_0)$.
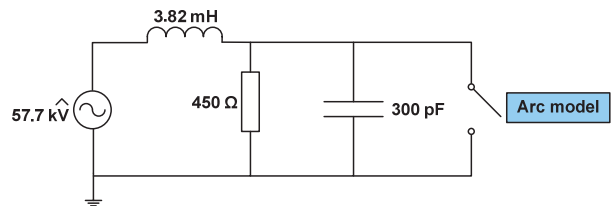

Fig. 2. Test circuit and arc model parameters: P_0=4 MW and β=0.68; T_0=1.5 μs and α=0.17 [9]

The initial values of $P(g_0)$ and $T(g_0)$ are also calculated for the conductance initial value. The low initial value of arc resistance at the time step t_0 was assumed and the conductance in the next time step was calculated from equation (4) in MODEL section of the ATP-EMTP. The output value from MODEL section is resistance and it is used as input value for nonlinear resistance component R(TACS) Type 91. A time step in ATP-EMTP has to be fixed and in some cases the selection of a very small time step leads to numerical problems and can prolong computation time. The calculated post zero arc current and peak value of the arc voltage were compared to three different models described in [9].

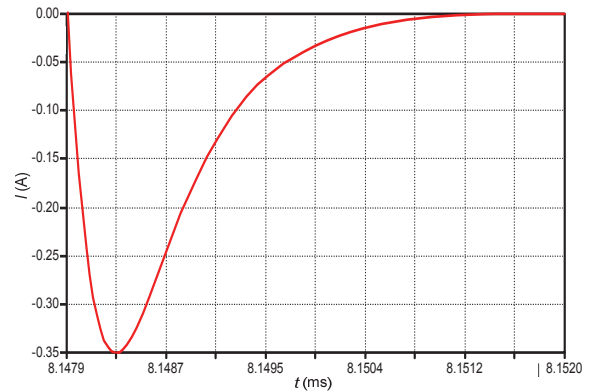The comparison of results is shown in Figs. 3-6.

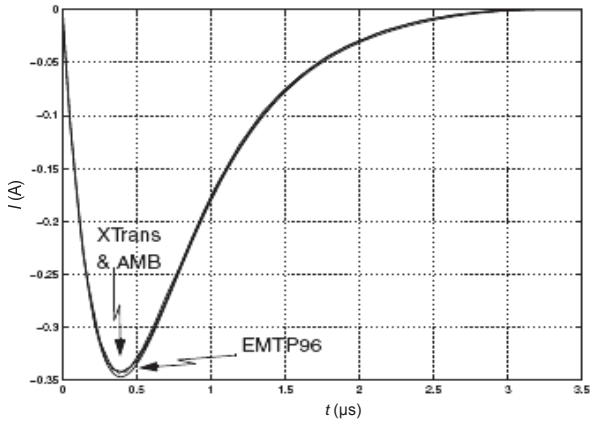Fig. 3. Calculated post arc current I_{max}=-0.35 A

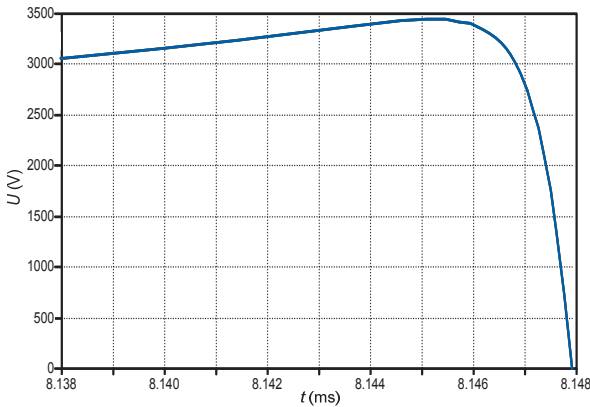Fig. 4. Post arc current – comparison with reference models [9]
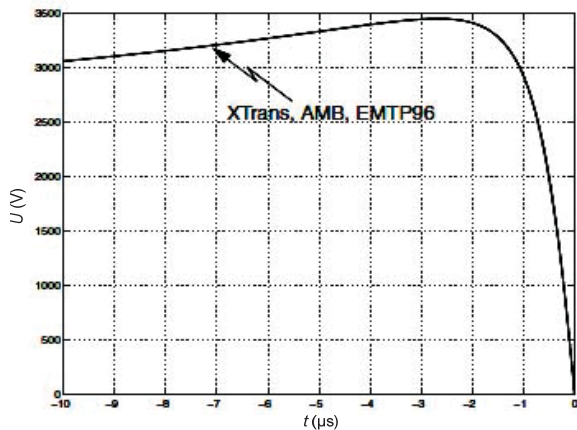

Fig. 5. Calculated arc voltage U_{max}=3442 V

Fig. 6. Arc voltage – comparison with reference models [9]

IV. Modeling of Substation and Transmission Line

The model of high frequency reactors that are installed in two phases (A and B) is depicted in Fig. 7. The capacitor voltage transformer in line bay compensates the high frequency reactor used for communication. The whole substation and transmission line depicted in Fig. 8 were modeled in detail (Fig. 9).

On the line side of the CB following devices were modeled with their stray capacitances: current transformer (CT) 680 pF; capacitor voltage transformer (CVT) 4400 pF; inductive voltage transformer 550 pF; and disconnector 200 pF [10].
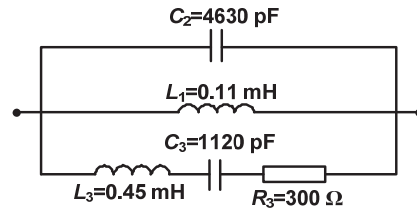

Fig. 7. High frequency reactor model

On the source side of the CB the main busbar system was modeled with LCC-JMarti model [11], and post insulators with capacitances to the ground. The equivalent network, which consisted of two line bays and two transformer bays, was represented by a voltage source and a short-circuit impedances.

V. Calculation of SLF According to IEC

A 400 kV CB with the rated short-circuit breaking current of 40 kA$_{rms}$ should be able to interrupt the short-circuit current of 36 kA$_{rms}$ in the cycle L90 (90% of the rated short-circuit breaking current) if subjected to the TRV, as it is proscribed by the IEC, with the rate of rise of about 7.2 kV/μs.

This rate of rise can be easily calculated using analytical expressions given in [6]. The short-circuit current of 40 kA in the substation was determined by adjusting the equivalent network on the source side of the CB. Short circuit calculations were performed at different distances from the substation in order to determine the RRRV at the current of 36 kA.

The "critical distance" of a fault location from the substation in the cycle L90 was used for the testing of interrupting capability of CB. Fault location at which RRRV is the highest was determined using the ATP simulations. A total of 12 simulations of single-phase SLF in phase A at various distances from the substation were conducted. The short circuit occurs at the time instant t=0 s, when the voltage in phase A has the maximum value.

For SFL at the "critical distance" of 1000 m from the substation (short-circuit current 36 kA), the RRRV on the line side and the CB equal 5.8085 kV/μs and 5.5810 kV/μs, respectively. The RRRV computed with EMTP differs from the one obtained by IEC due to detailed modeling of the substation. If the fault distance is greater than 2000 m, the RRRV and the short-circuit current decrease.

Also, for all distances shorter than 2000 m RRRV decreases, and short-circuit current increases (Figs. 10 and 11).
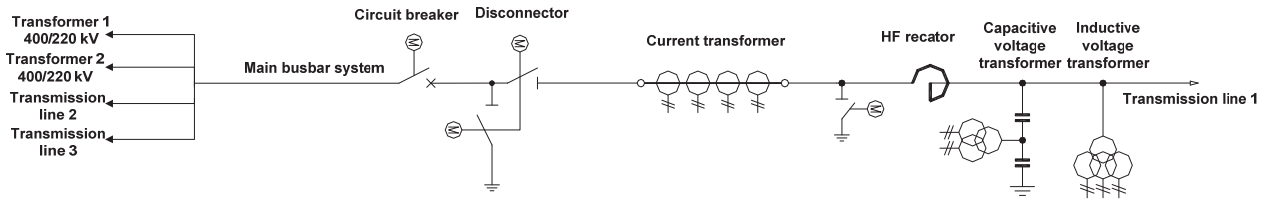
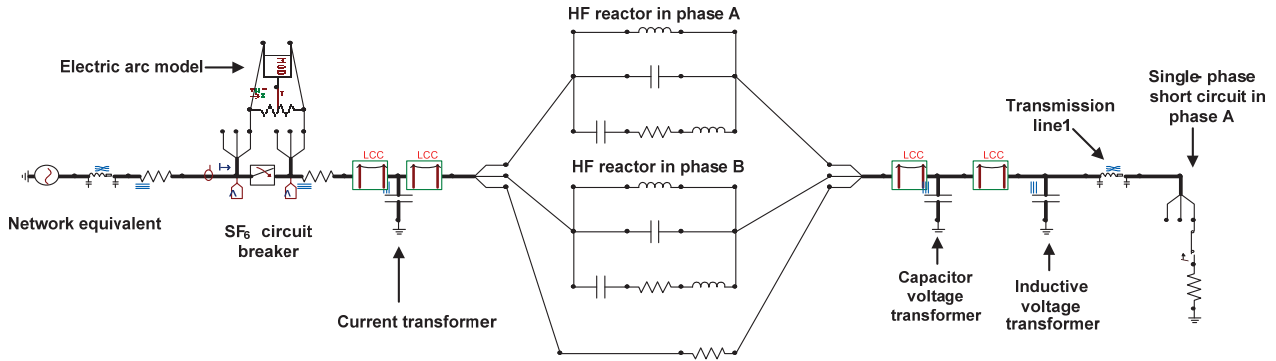Fig. 8. 400 kV line bay

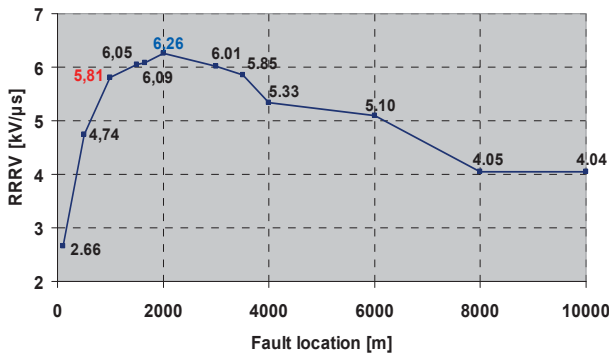Fig. 9. Three-phase model for TRV calculation of SLF according to IEC
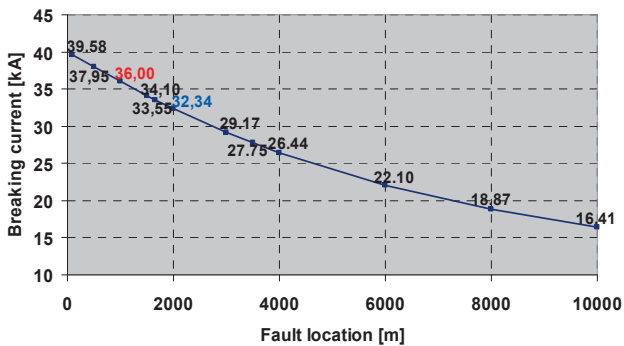

Fig. 10. RRRV value versus distance of SLF

Fig. 11. Breaking current versus distance of SLF

The maximum RRRV on the line side is 6.0702 kV/µs if the SLF occurs at the distance of 2000 m (short-circuit current 32.34 kA); as shown in Fig. 12. Fig. 13 shows the transient voltage on the CB with the maximum value of U_{max}=-515 kV.

VI. Calculation of SLF in an actual system

The calculation of SLF was conducted in order to obtain RRRV values in real operating conditions and the full operating state was assumed. For SLF at the distance of 1000 m with the fault current of 8.76 kA$_{rms}$ (Fig. 15), the RRRV on the line side and on the CB equal 1.3418 kV/µs and 1.3620 kV/µs (Fig. 14), respectively.

Simulations were performed for different SLF locations. The maximum values of RRRV were found for the fault current of 8.43 kA$_{rms}$ at the distance of 2000 m. In the real operating conditions (Fig. 18) the SLF currents exhibit values lower than the rated short-circuit breaking current. The RRRV on the line side and the CB were 1.6943 kV/µs (Fig. 16) and 1.7618 kV/µs, respectively. In this case TRV on the CB is U_{max}=670 kV (Fig. 17).
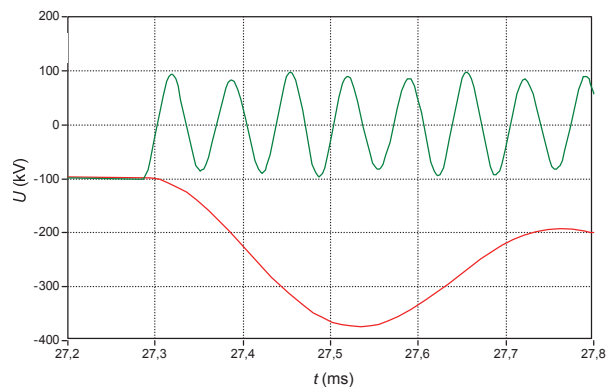

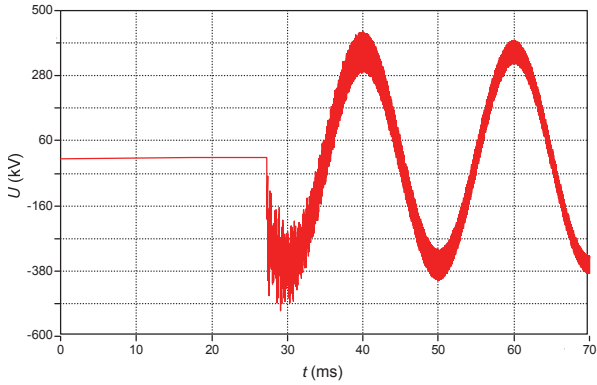Fig. 12. TRV on the line side RRRV=6.0702 kV/µs (green) and on the source side (red)
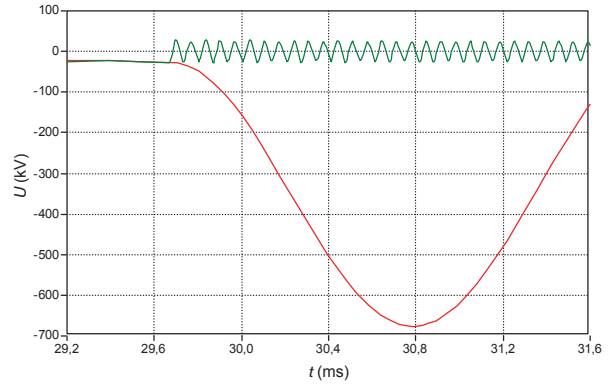
Fig. 13. TRV for 32.34 kA on CB; U_{max}=-515 kV

Fig. 14. RRRV value versus distance of SLF

Fig. 15. Breaking current versus distance of SLF

Fig. 16. TRV on the line side (green) RRRV=1.6943 kV/μs and on the source side (red)
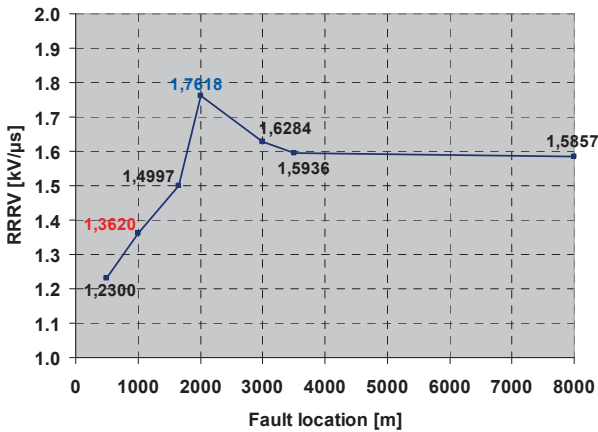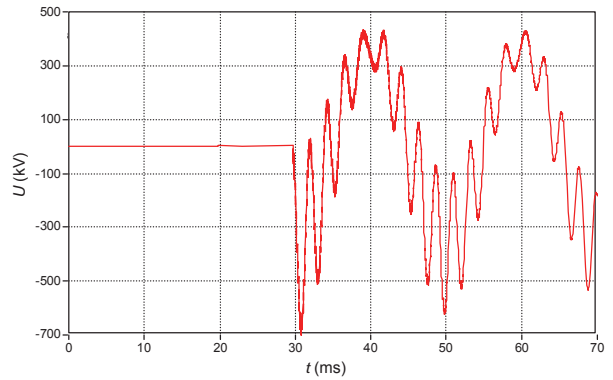
Fig. 17. TRV for 8.43 kA on CB; U_{max}=-670 kV
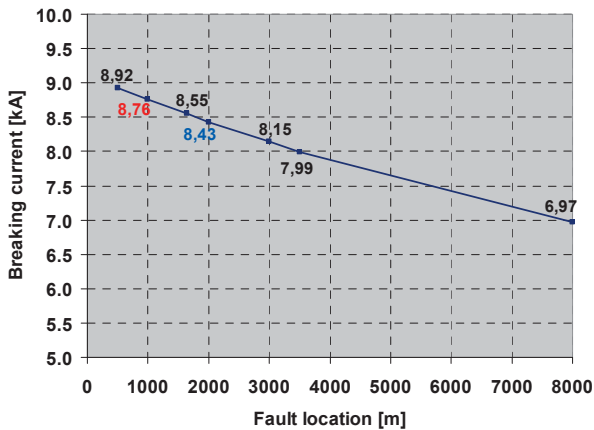
VII. Influence of the Distance of CVT from CB on TRV Steepness

The impact on the RRRV of the distance between the CB and the CVT with stray capacitance of 4400 pF was investigated. In reality, the CVT is located approximately 37 m from the CB and the SFL at the distance of 1000 m was analyzed. The results of the RRRVs for various distances are shown in Fig. 19.

From the results of these simulations it can be concluded that the RRRV on CB reduces with smaller distances between the CB and CVT. At the distance of 30 m the RRRV is minimal and it increases with the further reduction of distance.
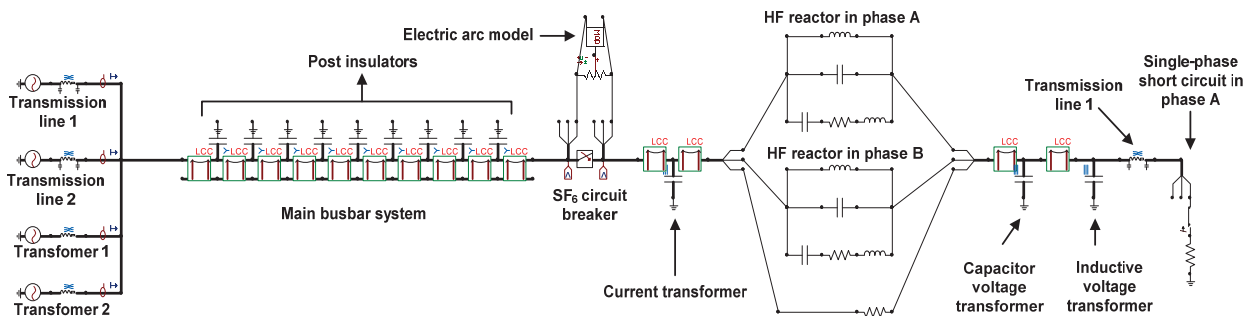

Fig. 18. Three-phase model of an actual system for TRV calculation in conditions of SLF
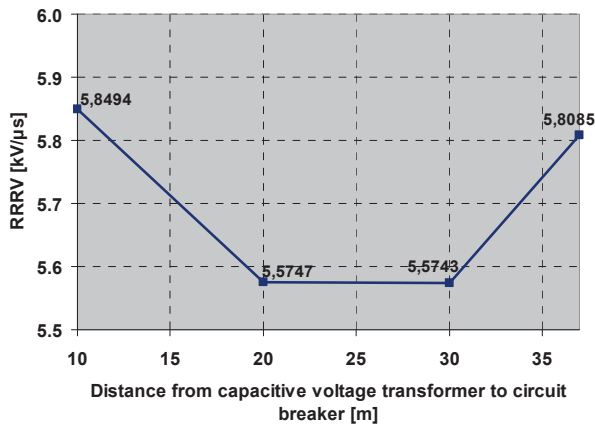
Fig. 19. RRRV versus distance between inductive voltage transformer and CB

VIII. Influence of Grading Capacitors on TRV

Modern SF$_6$ CBs are equipped with capacitors connected in parallel to CB terminals in order to equalize the voltage distribution and to decrease the RRRV on the CB contacts. Their influence was analyzed in the case of SLF at the distance of 2000 m from the substation for the fault current of 32.34 kA$_{eff}$. The results of these calculations are shown in Fig. 20.
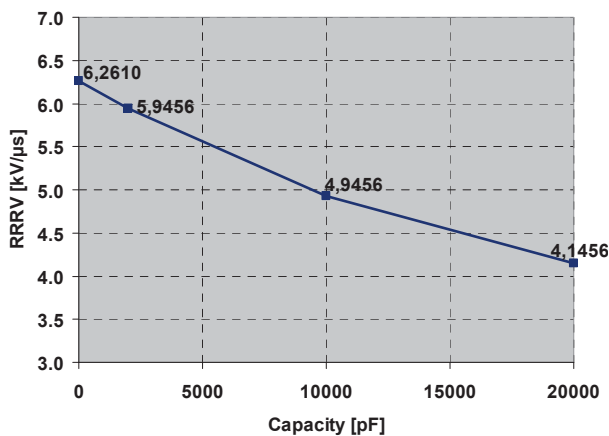

Fig. 20. RRRV versus capacity of grading capacitors

IX. Conclusion

TRV is calculated using EMTP-ATP software and a comparison of results obtained according to IEC procedure is performed.

The modeling of the arc resistance in a SF$_6$ CB is important, because it has a significant impact on the initial part of TRV. The Schwarz-Avdonin model was implemented in ATP-EMTP for a mathematical description of the electrical behavior of an electrical arc.

A 400 kV CB with the rated short-circuit breaking current of 40 kA$_{rms}$ should be able to interrupt the short-circuit current of 36 kA$_{rms}$ in the cycle L90 if subjected

to the TRV, as it is proscribed by the IEC, with the rate of rise of about 7.2 kV/µs.

According to conducted computer simulations for the short-circuit current of 36 kA$_{rms}$ rate of rise on CB was 5.81 kV/µs at the fault distance of 1000 m. The RRRV computed with ATP differs from the one obtained by IEC procedure due to the detailed modeling of the substation and the electric arc.

The fault location at which the rate of rise is the highest was determined using the EMTP-ATP simulations. The maximum calculated rate of rise was 6.26 kV/µs for the fault current of 32.34 kA at the distance of 2000 m. In the real operating conditions short-circuit currents are lower and maximum calculated rate of rise was 1.7618 kV/µs at the current of 8.43 kA and distance of 2000 m. RRRV on the CB reduces with the reduction of distances between the CB and the CVT up to 30 m and it increases with further reduction of distance.

The interrupting capability of the CB in SLF conditions is greatly increased with the additional capacitors installed in parallel to the CB terminals, due to the reduction of RRRV.

References

[1] Ruben D. Garzon, "High Voltage Circuit Breakers, Design and Applications", Dekker, ISBN: 0-8247-9821-X.
[2] Charles L. Wagner, Denis Dufournet, Georges F. Montillet, "Revision of the Application Guide for Transient Recovery Voltage for AC High-Voltage Circuit Breakers of IEEE C37.011", A Working Group Paper of the High Voltage Circuit Breaker Subcommittee, *IEEE Transactions on Power Delivery*, Vol.. 22, No. 1, January 2007.
[3] A. H. Soloot, A. Gholami, K. Niayesh, "Study on Post Arc Current and Transient Recovery Voltage in Vacuum Circuit Breaker", *International Review on Modelling and Simulations (IREMOS), vol. 4 n. 2*, April 2011, pp. 699-709.
[4] J. Moshtagh, S. Ghaderpour, "A New Modeling Approach for the Arcing Fault in Power Distribution Networks Using Lab Results", *International Review on Modelling and Simulations (IREMOS), vol. 4 n. 2*, April 2011, pp. 759-765.
[5] H. S. Park, J. W. Woo, J. W. Kang, K. S. Han, S. O. Han, "Analyzing TRV of CB When Installing Current Limit Reactors in UHV Power Systems", *International conference on power system transients (IPST)*, Lyon, 2007.
[6] IEC 62271-100: "High-voltage switchgear and controlgear", High-voltage alternating-current circuit-breakers, 2003.
[7] R. W. Alexander, D. Dufournet, "Transient recovery voltages (TRVs) for high-voltage circuit breakers", *IEEE Tutorial*, October 16th 2008, Calgary, Canada.
[8] CIGRE, Working Group 13.01 of the Study Committee 13, "State of the Art of Circuit-Breaker Modelling", December 1998.
[9] P. H. Schavemaker, L.Van Der Sluis, "The Arc model Blockset", *Proceedings of the Second IASTED International Conference, Power and Energy Systems (EuroPES)*, June 25-28, 2002, Crete, Greece.
[10] Ali F. Imece, D. W. Durbak, H. Elahi, S. Kolluri, A. Lux, D. Mader, T. E. McDemott, A. Morched, A. M. Mousa, R. Natarajan, L. Rugeles, and E. Tarasiewicz, "Modeling guidelines for fast front transients", Report prepared by the Fast Front Transients Task Force of the IEEE Modeling and Analysis of System Transients Working Group, *IEEE Transactions on Power Delivery*, Vol. 11, No. 1, January 1996.
[11] L. Prikler, H. K. Høidalen, "*ATP Draw User's Manual*", SEfAS TR A4790, ISBN 82-594-1358-2, Oct. 1998.

Authors' information

[1]Faculty of Electrical Engineering and Computing,
Department of High Voltage and Power Systems,
University of Zagreb,
Unska 3, HR-10000 Zagreb,
Croatia.

[2]Končar Electrical Engineering Institute,
Transformer Department,
High Voltage Laboratory,
Fallerovo šetalište 22, HR-10002 Zagreb,
Croatia.

Božidar Filipović-Grčić (M'10) was born in Sinj, Croatia, in 1983. He received his B.Sc. degree from the Faculty of Electrical Engineering and Computing, University of Zagreb, in 2007. Presently he is working at Faculty of Electrical Engineering and Computing (Department of High Voltage and Power Systems) and following doctoral studies. His areas of interest include power system transients, insulation co-ordination and high-voltage engineering. He is a member of IEEE society and Croatian Committee of CIGRÉ.

Ivo Uglešić (SM'08) was born in Zagreb, Croatia, in 1952. He received Ph.D. degree from the Faculty of Electrical Engineering and Computing, University of Zagreb, Croatia, in 1988. Presently, he is a Professor at the Faculty of Electrical Engineering and Computing (Department of High Voltage and Power Systems), University of Zagreb. Dr. Uglešić is the head of High-Voltage Laboratory at the Faculty of Electrical Engineering and Computing. His areas of interest include high-voltage engineering and power transmission.

Dalibor Filipović-Grčić was born in Sinj, Croatia, in 1980. He received his Ph.D. from the Faculty of Electrical Engineering and Computing, University of Zagreb, in 2010. Presently he is the head of High Voltage Laboratory at Končar Electrical Engineering Institute (Transformer department). His areas of interest include optimization of condenser type oil-paper insulation and high-voltage laboratory testing. He is a member of technical committees HZN/TO E 38 Instrument Transformers and HZN/TO E 42 High voltage test techniques.